This full text paper was peer reviewed at the direction of IEEE Communications Society subject matter experts for publication in the IEEE Secon 2010 proceedings.

Connectivity in Wireless Underground Sensor Networks

Zhi Sun and **Ian F. Akyildiz**

Broadband Wireless Networking Laboratory (BWN Lab)
School of Electrical & Computer Engineering, Georgia Institute of Technology, Atlanta, GA, 30332, USA
Email: {zsun; ian}@ece.gatech.edu

***Abstract*—This paper investigates the probabilistic connectivity of the Wireless Underground Sensor Networks (WUSNs). Due to the unique channel characteristics and the heterogeneous network architecture of the WUSNs, the connectivity analysis is much more complicated than in the terrestrial wireless sensor networks and ad hoc networks. To our knowledge, this connectivity problem in WUSNs was not addressed before. In this paper, a mathematical model is developed to analyze the probabilistic connectivity in WUSNs, which captures the effects of environmental parameters such as the soil moisture and soil composition, and system parameters such as the operating frequency, the sensor burial depth, the sink antenna height, the density of the sensor devices, the tolerable latency of the networks, and the number and the mobility of the above-ground sinks. The lower and upper bounds for the connectivity probability are derived analytically. Simulation studies are performed, where the theoretical bounds are validated, and the effects of several environmental and system parameters on the performance of these networks are investigated.**

I. Introduction

Wireless Underground Sensor Networks (WUSNs) are one important extension of the terrestrial wireless sensor networks, where the sensor nodes are buried underground and communicate wirelessly through soil. As a promising field, WUSNs enable a wide variety of novel applications, such as intelligent irrigation, sports field maintenance, border patrol, infrastructure monitoring, intruder detection, among of others [1], [2].

The connectivity as a fundamental property of wireless networks is essential for network functionalities. Because of the unique channel characteristics and the heterogeneous network architecture of the WUSNs, the connectivity analysis is much more complicated than in the terrestrial wireless sensor networks and ad hoc networks. In particular, since WUSNs consist of underground (UG) sensor nodes and aboveground (AG) data sinks [1], [3], [4], three different communication channels exist in WUSNs based on the locations of the transmitter and the receiver, including: underground-to-underground (UG-UG) channel, underground-to-aboveground (UG-AG) channel, and aboveground-to-underground (AG-UG) channel. The transmission range in these three different channels is different from each other. For the UG-UG channel, the transmission range is very limited compared to the terrestrial air channel [5], [6] due to the material absorption of the soil medium. For the UG-AG channel, the transmission range is much longer than the UG-UG channel [3], [4], [6]. This is because a large portion of the radiation energy can penetrate the air-ground interface from the soil to the air, and the path loss in the air is much smaller than that in the soil. For the AG-UG channel, the transmission range is much smaller than the UG-AG channel [6] since most of the radiation energy is reflected back when penetrating the air-ground interface from the air to the soil. Moreover, the transmission ranges in these three channels are also significantly impacted by the changes in soil moisture, soil composition, sensor burial depth, and radio operating frequency [1], [5], [6].

According to the channel characteristics and the envisioned applications of WUSNs, a practical WUSN network consists of underground sensors deployed in the sensing field, fixed above-ground data sinks set around the sensing field, and mobile data sinks carried by people or machineries inside the sensing field. Specifically, if there is only one single AG data sink, a prohibitively high density of UG sensors is required to guarantee the full connectivity, due to the small and dynamic transmission range of the UG-UG channel. If the cost of deployment and maintenance is considered, the extremely high density of UG sensors is unacceptable. To solve this problem, multiple AG sinks can be introduced [1], [3]. However, it is not desirable to deploy numerous AG devices inside the sensing field. For example, the AG devices inside a crop field may prevent large agricultural machinery to work; those AG devices may also prevent players to perform freely in a sport field. Hence, fixed AG sinks are only allowed to be deployed outside (around) the field under monitoring. This constraint causes that the sensor density far from the field border is still prohibitively high. One feasible solution is to let the agricultural machineries or the users inside the field carry receiver devices and perform as mobile data sinks [1]. The mobile sink moves randomly in the sensing field, and collects data from the UG sensors when moving into their transmission range. Therefore, if the WUSN applications can tolerate a certain level of latency, the UG sensors far from the region border do not need to connect to a fixed sink but can expect a mobile sink coming and collecting their data.

A terrestrial wireless sensor network is defined to be fully connected if every sensor is connected to at least one data sink in a multi-hop fashion [11]. This is different from the ad hoc networks if multiple data sinks exist. Moreover, if the mobile data sinks are introduced, the probability that a sensor is connected to at least one sink increases with the increasing latency tolerance. It follows that there is a tradeoff between the high connectivity probability and low latency. Consequently, we introduce the following definitions:

Definition 1: In a WUSN, a UG sensor is connected if either of the following statements is true.

- *The UG sensor is connected to a fixed AG sink in a multi-*

978-1-4244-7151-5/10/$26.00 ©2010 IEEE

hop fashion;

- *The UG sensor is connected to a mobile AG sink at least once in a multi-hop fashion within the duration t, where t is the maximum tolerable latency.*

Definition 2: A WUSN is fully connected if all its UG sensors are connected.

The connectivity analysis in WUSNs is a complicated problem since there are three types of sensor nodes (UG sensors, AG fixed sinks and AG mobile sinks) in two different mediums (soil and air) with three different transmission ranges (UG-UG, UG-AG and AG-UG). Additionally, the transmission ranges are highly dynamic due to the changes of the environmental parameters as well as the radio frequency and the burial depth. Besides, since the channel between AG and UG devices is asymmetrical, the network connectivity is also asymmetrical. Moreover, the tradeoff between the good connectivity and the low latency needs to be considered due to the use of mobile sinks. To the best of our knowledge, these problems have not been addressed in existing works so far.

In this paper, we analyze the connectivity in WUSNs by taking into consideration both the unique channel characteristics and the heterogeneous network architecture. The solution will provide guidelines to design the system parameters for WUSNs according to the environmental conditions. The lower bound and upper bounds of the connectivity probability are derived analytically as functions of the radio power, the operating frequency, the UG sensor burial depth, the AG sink antenna height, the density of the sensor devices, the soil moisture and soil composition, the tolerable latency of the networks, and the number and the mobility of the mobile sinks. Those theoretical probability bounds are validated by simulations. The effects of various environmental and system parameters are analyzed quantitatively.

The remainder of this paper is organized as follows. In Section II, the related works are introduced. In Section III, the channel, network and mobility models are described. Next, the lower bound and the upper bound of the connectivity probability in WUSNs are derived in Section IV and Section V, respectively. Then, in Section VI, simulation studies are performed. Finally, the paper is concluded in Section VII.

II. Related Work

In the past few years, the connectivity in the homogenous ad hoc networks has been well analyzed thoroughly. In [7], the necessary and sufficient scaling of the transmission range is analyzed to achieve the full connectivity. In [8], the upper bound of the connectivity probability is proposed as a function of the node density. Comprehensive simulation results for the connectivity in mobile ad hoc network are provided in [9]. For heterogeneous ad hoc networks, it is proven in [10] that the connectivity of ad hoc networks can be improved by using base stations in certain conditions.

In [11], the connectivity in a sensor network with node sleeping scheme is analyzed. However, the authors assume that only one data sink exists. Therefore the connectivity criteria is the same as in the ad hoc networks. In [12], multiple sinks are considered in the connectivity analysis in wireless sensor networks. However, the authors assume that the sensors can be connected to the sinks only in a single-hop fashion. Additionally, multiple sinks are distributed across the entire sensing field, which is not feasible in many applications, especially in WUSNs.

To date, no existing work has addressed the connectivity problems in WUSNs. The problems include: 1) the connectivity probability of a multi-hop wireless sensor network over a bounded region when multiple data sinks are deployed along the border of the region, 2) the influence of the asymmetric and dynamic channels on the network connectivity, and 3) the tradeoff between the connectivity and the latency if mobile data sinks exist. In this paper, we develop the solutions for these problems by using the particular channel characteristics of the WUSNs [1], [5].

III. Preliminaries

A. Channel Model

The channel model for WUSNs is first developed in [5], and has been validated and extended in [3], [6]. In this section, we calculate the transmission ranges of the three channels in WUSNs based on the channel models proposed in [2], [3], [5]. Since the WUSNs are mainly deployed in spacious fields (e.g. crop field or sports field), the multi-path fading effects can also be ignored. Moreover, we assume that the interference problem is addressed by a proper MAC protocol for WUSNs.

1) UG-UG Channel: Assuming that $L_{UG}(d)$ is the signal loss of an underground soil path with length d (meters), then [2], [5]

$$L_{UG}(d) = 6.4 + 20\log d + 20\log\beta + 8.69\alpha d\,, \tag{1}$$

where α is the attenuation constant whose unit is $1/m$, and β is the phase shifting constant whose unit is $radian/m$. The values of α and β depend on the dielectric properties of soil:

$$\begin{aligned}\alpha &= 2\pi f\sqrt{\frac{\mu\epsilon'}{2}\left[\sqrt{1+(\frac{\epsilon''}{\epsilon'})^2}-1\right]},\\ \beta &= 2\pi f\sqrt{\frac{\mu\epsilon'}{2}\left[\sqrt{1+(\frac{\epsilon''}{\epsilon'})^2}+1\right]},\end{aligned} \tag{2}$$

where f is the operating frequency, μ is the magnetic permeability, ϵ' and ϵ'' are the real and imaginary parts of the relative dielectric constant of soil-water mixture. ϵ' and ϵ'' are functions of the soil properties, which include the volumetric water content (VWC) of the mixture, the bulk density, and the composition of soil in terms of sand and clay fractions. The detailed expressions of ϵ' and ϵ'' can be found in [2], [5].

Since the UG sensors are buried near the air-ground interface (the burial depth is less than 2 m), the reflection from the air-ground interface needs to be considered. If the burial depth of UG sensors is h_u, the total path loss of the UG-UG channel L_{UG-UG} is deduced as [2], [5]:

$$L_{UG-UG} = L_{UG}(d) - 10\log V(d, h_u)\,, \tag{3}$$

where $V(d,h)$ is the attenuation factor due to the second path:

$$\begin{aligned}V^2(d) =& 1 + (\Gamma\cdot\exp(-\alpha\Delta r))^2\\ &- 2\Gamma\exp(-\alpha\Delta r)\cos\left(\pi-\left(\phi-\frac{2\pi f}{c\sqrt{\epsilon'}}\Delta r\right)\right)\,,\end{aligned}$$

where Γ and ϕ are the amplitude and phase angle of the reflection coefficient at the reflection point, c is the velocity

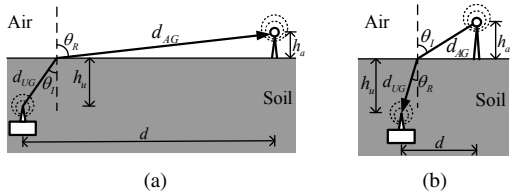

(a) (b)

Fig. 1. Illustration of (a) UG-AG channel and (b) AG-UG channel

of light in vacuum, and $\Delta r = \sqrt{d^2/4 + h_u^2} - d$, is the difference of the two paths.

Assuming that the transmit power of the UG sensor is P_t^u, the antenna gains of the receiver and transmitter are g_r and g_t. Then the received power, P_r^{U2U}, at a receiver sensor node d meters away is $P_r^{U2U} = P_t^u + g_r + g_t - L_{UG-UG}$. Consequently, the transmission range of the UG-UG channel is:

$$R_{UG-UG} = \max\{d : P_r^{U2U}/P_n > SNR_{th}\}\,, \tag{4}$$

where P_n is the noise power; and SNR_{th} is the minimum signal-to-noise ratio required by the receiver.

2) UG-AG Channel: The path loss of the UG-AG channel L_{UG-AG} consists of three parts: the UG path loss L_{UG}, the AG path loss L_{AG} and the refraction loss from soil to air L_{UG-AG}^R:

$$L_{UG-AG} = L_{UG}(d_{UG}) + L_{AG}(d_{AG}) + L_{UG-AG}^R\,, \tag{5}$$

where d_{UG} is the length of the UG path, and the d_{AG} is the length of the AG path, as shown in Fig. 1(a). The UG path loss L_{UG} can be derived from (1). The AG path loss L_{AG} is:

$$L_{AG}(d) = -147.6 + 20\log d + 20\log f\,, \tag{6}$$

Since the dielectric constant of soil is much larger than the air, the signals with an incident angle θ_I that is larger than the critical angle θ_c will be completely reflected. Moreover, because the length of the AG path d_{AG} is much larger than the height of the AG sink antenna h_a, the incident angle θ_I is approximately equal to θ_c; and the refracted angle θ_R is approximately equal to 90°, as shown in Fig. 1(a). Then the horizontal distance d between the UG sensor and AG sink is approximately equal to d_{AG}. And

$$d_{UG} \simeq \frac{h_u}{\cos\theta_c}; \quad \theta_c \simeq \arcsin\frac{1}{\sqrt{\epsilon'}}. \tag{7}$$

The refraction loss L_{UG-AG}^R can be calculated as:

$$L_{UG-AG}^R \simeq 10\log\frac{(\sqrt{\epsilon'}+1)^2}{4\sqrt{\epsilon'}}. \tag{8}$$

Then the received power is $P_r^{U-A} = P_t^u + g_r + g_t - L_{UG-AG}$ at the AG sink. Consequently the transmission range of the UG-AG channel is calculated as:

$$R_{UG-AG} \simeq \max\{d_{AG} : P_r^{U-A}/P_n > SNR_{th}\}\,. \tag{9}$$

3) AG-UG Channel: Similar to the UG-AG channel, the path loss of the AG-UG channel is:

$$L_{AG-UG} = L_{UG}(d_{UG}) + L_{AG}(d_{AG}) + L_{AG-UG}^R\,, \tag{10}$$

where L_{AG-UG}^R is the refraction loss from air to soil. As shown in Fig. 1(b), because the dielectric constant of soil is much larger than the air, most radiation energy from the AG sink will be reflected back if the incident angle θ_I is large. Therefore, we only consider the signal with small incident angle. Consequently, the refracted angle θ_R in the soil is even smaller hence it can be viewed approximately as zero. Then the UG path length $d_{UG} \simeq h_u$, and the horizontal distance d between the UG sensor and AG sink is:

$$d \simeq \sqrt{d_{AG}^2 - h_a^2}\,, \quad \cos\theta_I = \frac{h_a}{d_{AG}}\,. \tag{11}$$

The refraction loss L_{AG-UG}^R can be calculated as:

$$L_{AG-UG}^R \simeq 10\log\frac{(\cos\theta_I + \sqrt{\epsilon' - \sin^2\theta_I})^2}{4\cos\theta_I\sqrt{\epsilon' - \sin^2\theta_I}}\,. \tag{12}$$

If the transmit power of the AG sink is P_t^a, then the received power is $P_r^{A-U} = P_t^a + g_r + g_t - L_{AG-UG}$ at the UG sensor. Therefore the transmission range of the UG-AG channel is calculated as:

$$R_{AG-UG} \simeq \max\{d : P_r^{A-U}/P_n > SNR_{th}\}\,. \tag{13}$$

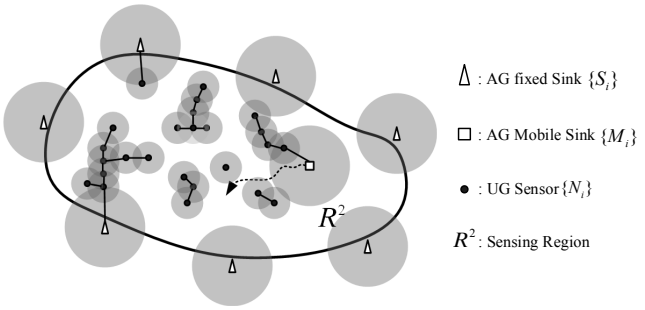

Fig. 2. The network model of the WUSNs. The gray disk is the range in which other nodes can connect to the node in the center of the disk.

B. Network Model

As shown in Fig. 2, the WUSN is deployed in a bounded region $\mathbb{R}^2$. The UG sensors $\{N_i, i = 1, 2, \cdots\}$ are distributed inside the region $\mathbb{R}^2$ according to a homogeneous Poisson point process of constant spatial intensity λ. There are n fixed AG sinks $\{S_i, i = 1, 2, \cdots n\}$ uniformly distributed along the border of the sensing region $\mathbb{R}^2$. Moreover, there are m mobile AG sinks $\{M_i, i = 1, 2, \cdots m\}$ carried by people or machineries inside the sensing region. In this paper, we analyze the probability of the full connectivity in WUSNs. The definition of the full connectivity in WUSN is given in Section I. The sensing region $\mathbb{R}^2$ is much larger than the transmission range of the UG sensors. Hence the scale of the network is large and the border effects can be ignored.

The functionalities of the WUSNs include two phases: the sensing phase and the control phase. In the sensing phase, the UG sensors report sensing data to the AG sinks, while in the control phase, the AG sinks send control messages to the UG sensors. Since the UG-AG channel and the AG-UG channel are asymmetrical, we analyze the connectivity in the two phases separately. In the sensing phase, the UG-UG and the UG-AG channels are used, while in the control phase UG-UG and the AG-UG channel are utilized. The maximum tolerable latencies in the sensing phase and control phase are t_s and t_c, respectively. $t_s \ll t_c$ in most envisioned applications. Since the

only difference between the connectivity analysis in the two phases is the transmission ranges and the tolerable latencies, we calculate the connectivity probability in the sensing phase in the next two sections. The connectivity probability in the control phase can be derived from the developed formulas by simply replacing the transmission range and the tolerable latency.

C. Mobility Model

Since the mobile sinks in above-ground are carried by people or machineries, their mobility can be modeled as the random walk [13]. The random walk model of a mobile data sink is defined by a sequence of steps. A step consists of a flight with a random direction followed by a pause. The initial position of each mobile sink is uniformly distributed in the sensing region $\mathbb{R}^2$. If the initial position of a mobile sink is (x_0, y_0), the position of this mobile sink after time t, (x_t, y_t), follows a joint Gaussian distribution. The probability density function (PDF) of the position of the mobile sink can be expressed as:

$$P\Big(t,(x_t,y_t)\Big) = \frac{1}{2\pi t\sigma^2/\tau}\exp\left(-\frac{(x_t-x_0)^2+(y_t-y_0)^2}{2t\sigma^2/\tau}\right), \quad (14)$$

where σ^2 is the variance of the flight length and τ is mean value of the step time. Larger σ^2 and smaller τ indicate that the mobile sink is more active.

IV. Lower Bound of the Connectivity Probability in WUSNs

According to the above channel characteristics, the network and mobility models, the probability that the WUSNs are fully connected depends on various environmental and system parameters. Here and in the next section, the lower and upper bounds for the connectivity probability are derived analytically. These theoretical bounds enable the quantitative analysis of the effects of multiple system and environmental parameters on the connectivity in WUSNs.

From Definition 2, the full connectivity probability P_c of WUSNs can be expressed as:

$$\begin{aligned} P_c &= P(\text{Every UG sensor is connected}) \\ &= \sum_{n=0}^{\infty} P(\text{All } n \text{ UG sensors are connected}) \\ &\qquad \times P(\text{There are } n \text{ UG sensors in } \mathbb{R}^2)\,. \end{aligned} \quad (15)$$

According to the FKG inequality [14],

$$P(\text{All } n \text{ UG sensors are connected}) \begin{cases} \geq \prod_{i=1}^{n} P(N_i \text{ is connected})\,, & \text{if } n \geq 1 \\ = 0\,, & \text{if } n = 0\,. \end{cases}$$

Since each UG sensor node is assumed to be identically distributed, then

$$\prod_{i=1}^{n} P(N_i \text{ is connected}) = P^n(N_i \text{ is connected})$$

Additionally, since the UG sensors are distributed according to a Poisson point process,

$$P(\text{There are } n \text{ UG sensors in } \mathbb{R}^2) = \frac{(\lambda S_{\mathbb{R}^2})^n}{n!}e^{-\lambda S_{\mathbb{R}^2}}\,, \quad (16)$$

where $S_{\mathbb{R}^2}$ is the area of the region $\mathbb{R}^2$. Then

$$\begin{aligned} P_c &\geq \sum_{n=0}^{\infty} P^n(N_i \text{ is connected}) \cdot \frac{(\lambda S_{\mathbb{R}^2})^n}{n!}e^{-\lambda S_{\mathbb{R}^2}} \\ &= \exp\Big\{\lambda S_{\mathbb{R}^2}\cdot[P(N_i \text{ is connected}) - 1]\Big\}\,. \end{aligned} \quad (17)$$

Next, we evaluate the lower bound of $P(N_i \text{ is connected})$ in (17), the probability that a single UG sensor node N_i is connected. Since the position of N_i is random, then

$$P(N_i \text{ is connected}) = \int_{S_{\mathbb{R}^2}} \frac{1}{S_{\mathbb{R}^2}} P(N_i^{(x_i,y_i)} \text{ is connected})\, dx_i dy_i\,,$$

where $N_i^{(x_i,y_i)}$ indicates that the position of N_i is (x_i, y_i).

The total directly covered area of the fixed AG sinks in region $\mathbb{R}^2$ is denoted as S_{fix}. Note that S_{fix} is determined since fixed AG sinks are stationary. If N_i is deployed in the coverage area, the connectivity probability is 1. Hence,

$$\begin{aligned} P(N_i \text{ is connected}) &= \frac{S_{fix}}{S_{\mathbb{R}^2}} \\ &\quad + \int_{S_{\mathbb{R}^2}-S_{fix}} \frac{1}{S_{\mathbb{R}^2}} P(N_i^{(x_i,y_i)} \text{ is connected})\, dx_i dy_i\,. \end{aligned} \quad (18)$$

From Definition 1,

$$P(N_i^{(x_i,y_i)} \text{is connected}) = P(A \cup B) \geq \max[P(A),\ P(B)], \quad (19)$$

where A is the event that the UG sensor $N_i^{(x_i,y_i)}$ connects to at least one fixed AG sink; B is the event that the UG sensor $N_i^{(x_i,y_i)}$ has connected to at least one mobile AG sink at least once within the tolerable latency t_s. Furthermore

$$P(A) \geq \max_{\mathbf{J}\in\{S_i\}} \Big[P(N_i^{(x_i,y_i)} \sim \text{Sink}_{\mathbf{J}})\Big]\,, \quad (20)$$

where $(N_i^{(x_i,y_i)} \sim \text{Sink}_{\mathbf{J}})$ indicates that the UG sensor $N_i^{(x_i,y_i)}$ connects to the fixed sink $\mathbf{J}$, and $\{S_i\}$ is the set of all fixed AG sinks. Similarly,

$$P(B) \geq \max_{\mathbf{K}\in\{M_i\}} \Big[P(N_i^{(x_i,y_i)} \sim \text{Sink}_{\mathbf{K}} \text{ in } t_s)\Big]\,, \quad (21)$$

where $(N_i^{(x_i,y_i)} \sim \text{Sink}_{\mathbf{K}} \text{ in } t_s)$ indicates that the UG sensor $N_i^{(x_i,y_i)}$ has connected to the mobile sink $\mathbf{K}$ at least once within duration t_s, $\{M_i\}$ is the set of all mobile AG sinks.

The event $(N_i^{(x_i,y_i)} \sim \text{Sink}_{\mathbf{K}} \text{ in } t_s)$ can be viewed as the union of infinitely many sub-events $\{C(t_i), i = 1, 2, \cdots\}$, so that

$$\begin{aligned} P(N_i^{(x_i,y_i)} \sim \text{Sink}_{\mathbf{K}} \text{ in } t_s) &= P[C(t_1) \cup C(t_2) \cup \cdots] \\ &\geq \max_{t_i}\Big\{P[C(t_i)]\Big\}\,, \end{aligned} \quad (22)$$

where $C(t_i)$ is the event that the UG sensor $N_i^{(x_i,y_i)}$ connects to the mobile sink $\mathbf{K}$ at time instant t_i, Note that $t_i \in [0, t_s]$, and $t_i \neq t_j$ if $i \neq j$. At each time instant, the mobile sink $\mathbf{K}$ can be considered to be static. Therefore, $\mathbf{K}$ can be viewed as a fixed AG sink at each time instant. Then

$$P[C(t_i)] = P(N_i^{(x_i,y_i)} \sim \text{Sink}_{\mathbf{K}(t_i)})\,, \quad (23)$$

where $\mathbf{K}(t_i)$ is the equivalent fixed sink that has the same position as the mobile sink $\mathbf{K}$ at time instant t_i. By substituting (22) and (23) into (21), we obtain

$$P(B) \geq \max_{\mathbf{K}\in\{M_i\}} \left\{\max_{t_i\in[0,t_s]} \Big[P(N_i^{(x_i,y_i)} \sim \text{Sink}_{\mathbf{K}(t_i)})\Big]\right\}\,. \quad (24)$$

Assume that t_{min} is the time instant when $\mathbf{K}$ is passing the point closest to $N_i^{(x_i,y_i)}$ on its motion trail. Then $\mathbf{K}(t_{min})$ is the closest equivalent fixed sink to $N_i^{(x_i,y_i)}$ among all equivalent fixed sinks of $\mathbf{K}$ during t_s. The distance between $N_i^{(x_i,y_i)}$ and $\mathbf{K}(t_{min})$ is denoted as $l_{mobi,\mathbf{K}}$.

According to the definition of the maximum function, (20) can be further derived as:

$$\max_{\mathbf{J}\in\{S_i\}}\left[P(N_i^{(x_i,y_i)} \sim \text{Sink}_{\mathbf{J}})\right] \geq P(N_i^{(x_i,y_i)} \sim \text{Sink}_{\mathbf{J}_{min}}), \quad (25)$$

where $\mathbf{J}_{min}$ is the fixed AG sink that is closest to the UG sensor $N_i^{(x_i,y_i)}$. The distance between $\mathbf{J}_{min}$ and $N_i^{(x_i,y_i)}$ is denoted as l_{fix}.

Similarly, (24) can be further written as:

$$\max_{\mathbf{K}\in\{M_i\}}\left\{\max_{t_i\in[0,t_s]}\left[P(N_i^{(x_i,y_i)} \sim \text{Sink}_{\mathbf{K}(t_i)})\right]\right\} \geq P(N_i^{(x_i,y_i)} \sim \text{Sink}_{\mathbf{K}_{min}(t_{min})}), \quad (26)$$

where $\mathbf{K}_{min}(t_{min})$ is the equivalent fixed sink that is the closest to the UG sensor $N_i^{(x_i,y_i)}$ of all mobile sinks at all time instances. Therefore, $l_{mobi,\mathbf{K}_{\min}} = \min\{l_{mobi,\mathbf{K}}, \mathbf{K} \in \{M_i\}\}$.

By substituting (20), (24), (25) and (26) into (19), we derive:

$$\begin{aligned} &P(N_i^{(x_i,y_i)} \text{ is connected}) \quad (27)\\ &\geq \max\left\{P(N_i^{(x_i,y_i)} \sim \text{Sink}_{\mathbf{J}_{min}}),\ P(N_i^{(x_i,y_i)} \sim \text{Sink}_{\mathbf{K}_{min}(t_{min})})\right\}. \end{aligned}$$

If $l_{mobi,\mathbf{K}_{\min}} \leq R_{UG-AG}$, then $N_i^{(x_i,y_i)}$ can connect to $\text{Sink}_{\mathbf{K}_{min}(t_{min})}$ directly. Then $P(N_i^{(x_i,y_i)} \sim \text{Sink}_{\mathbf{K}_{min}(t_{min})}) = 1$. Hence,

$$\begin{aligned} &\max\left\{P(N_i^{(x_i,y_i)} \sim \text{Sink}_{\mathbf{J}_{min}}),\ P(N_i^{(x_i,y_i)} \sim \text{Sink}_{\mathbf{K}_{min}(t_{min})})\right\}\\ &\geq P(N_i^{(x_i,y_i)} \sim \text{Sink}_{\mathbf{J}_{min}}) \cdot P(l_{mobi,\mathbf{K}_{\min}} > R_{UG-AG})\\ &\quad + P(N_i^{(x_i,y_i)} \sim \text{Sink}_{\mathbf{K}_{min}(t_{min})} \big| l_{mobi,\mathbf{K}_{\min}} > R_{UG-AG})\\ &\quad \cdot P(l_{mobi,\mathbf{K}_{\min}} \leq R_{UG-AG})\\ &= P(N_i^{(x_i,y_i)} \sim \text{Sink}_{\mathbf{J}_{min}}) \cdot P(l_{mobi,\mathbf{K}_{\min}} > R_{UG-AG})\\ &\quad + 1 \cdot [1 - P(l_{mobi,\mathbf{K}_{\min}} > R_{UG-AG})]. \quad (28) \end{aligned}$$

To calculate the probability in (28), two sub-problems need to be analyzed: 1) the lower bound of the probability that a sensor at (x_i, y_i) connects to a fixed sink at (x_j, y_j) in a multi-hop fashion, $P(N_i^{(x_i,y_i)} \sim \text{Sink}_j^{(x_j,y_j)})$; and 2) the first hit time problem of the random walk model.

A. Lower Bound of $P(N_i^{(x_i,y_i)} \sim Sink_j^{(x_j,y_j)})$

Assuming a UG sensor N_i is located at (x_i, y_i), and a fixed sink Sink_j is located at (x_j, y_j). To derive the lower bound of the probability that N_i connects to Sink_j, we first map the WUSN on a discrete lattice, as shown in Fig. 3.

In Fig. 3, the square lattice L over the region $\mathbb{R}^2$ is constructed as follows. The sensor N_i is on one vertex of the lattice, which is set as the origin of the lattice. The straight line ef connecting N_i and Sink_j forms a sequence of horizontal edges of the lattice L. The length of each edge is d. Let L' be the dual lattice of L. The vertexes of L' are placed in the center of every square of L. The edges of L' crosse every edge of L. According to the above structure, there exists a one-to-one relation between the edges of L and the edges of L'. L and L' have the same edge length $d = \frac{1}{\sqrt{5}}R_{UG-UG}$. The value is chosen so that two UG sensors deployed in two adjacent squares of the dual lattice L' are guaranteed to be able to connect to each other.

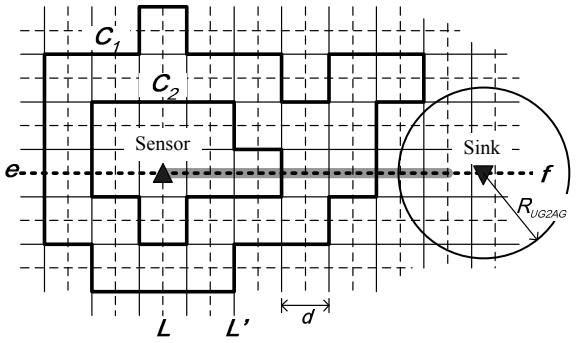

Fig. 3. Mapping the WUSN on a lattice **L** (dashed) and its dual **L'** (plain).

Definition 3: An edge l' of the L' is said to be open if both squares adjacent to l contains at least one UG sensor.

Definition 4: An edge l of the L is said to be open if and only if the corresponding edge of L' is open.

Definition 5: A path of the L or L's is said to be open (closed) if all edges forming the path are open (closed).

Therefore, if a open path of the L is given, all the UG sensors in the squares in L' along the open path belong to the same cluster and are connected to each other. The states of the edges (open or closed) are independent from each other. The probability that an edge is closed is denoted as q, which is the same in L and L'. q can be calculated according to the Poisson point process of the UG sensors. Hence,

$$q = P^2(\text{There is no sensor in a square } d^2) = e^{-2\lambda d^2}. \quad (29)$$

Now consider the connection between the sensor N_i and Sink_j. The region $\mathbb{R}^2$ is divided into two parts, the region inside the circle C_{sink} and the region outside the circle. C_{sink} is defined as the circle with radius R_{UG-AG} and center located at the position of Sink_j, as shown in Fig. 3. All UG sensors located inside C_{sink} connects to Sink_j directly. Note that $R_{UG-AG} \gg R_{UG-UG} = \sqrt{5}d$. If there is an open path of L connecting N_i and a vertex V of L inside C_{sink}, then N_i and Sink_j are guaranteed to be connected by each other. Note that the square in L' containing vertex V should be completely inside the circle C_{sink}. The set of these open paths is denoted as $\{P_o\}$, then

$$P(N_i^{(x_i,y_i)} \sim \text{Sink}_j^{(x_j,y_j)}) \geq P\left(\left|\{P_o\}\right| > 0\right) = 1 - P\left(\left|\{P_o\}\right| = 0\right), \quad (30)$$

where $\left|\{P_o\}\right|$ is the number of the open path P_o. Furthermore, $\left|\{P_o\}\right| = 0$, if and only if the sensor N_i lies in the interior of some closed circuits of the dual lattice L', which do not contain a whole common square that is also inside the circle C_{sink}, such as C_1 and C_2 (thick black circuits) in Fig. 3.

We now evaluate $P\left(\left|\{P_o\}\right| = 0\right)$ by counting the number of such closed circuits in L'. Let $\rho(n)$ be the number of circuits in L' which have length nd and contain the UG sensor N_i in their interiors. To contain N_i in their interiors, those circuits pass through some point on the line ef, as shown in Fig. 3. The position of the corresponding pass vertex in L' has the form of $(kd - \frac{1}{2}d, \frac{1}{2}d)$. k cannot be larger than $\lfloor \frac{n}{2} \rfloor - 1$. Otherwise the circuits would have a length larger than n. Thus, such a

circuit contains a self-avoiding walk of length $n-1$ starting from a vertex at $(kd-\frac{1}{2}d, \frac{1}{2}d)$ and $k > \lfloor \frac{n}{2} \rfloor - 1$. Moreover, to contain N_i inside, the length of the circuits $n \geq 4$. The number of self avoiding walks of L' having length n and beginning at a vertex is denoted as $\sigma(n)$. It has been proven in [14] that $\sigma(n) \leq 4 \cdot 3^{n-1}$ in a 2-D plane.

Since those closed circuits do not contain a whole common square with the circle C_{sink}, such as C_1 or C_2 in Fig. 3, they must pass through at least one point on the line segment on ef between the sensor N_i and the first vertex of L inside C_{sink}. This line segment is illustrated by the thick gray segment in Fig. 3. The length of the line segment is Wd. The distance between the sensor and the sink is denoted as D. If $D > R_{UG-AG}$,

$$\begin{aligned} W &= \lceil (D - R_{UG-AG})/d \rceil + 1 \\ &= \left\lceil \frac{\sqrt{(x_i - x_j)^2 - (y_i - y_j)^2} - R_{UG-AG}}{d} \right\rceil + 1 \ . \end{aligned} \tag{31}$$

Hence, those closed circuits contain a self-avoiding walk of length $n-1$ ($n \geq 4$) starting from a vertex at $(kd - \frac{1}{2}d, \frac{1}{2}d)$ and $k \leq \min\{\lfloor \frac{n}{2} \rfloor - 1, W\}$. The total number of such closed circuits is denoted as CN. Based on the above discussions, the upper bound of CN can be calculated as follows.

$$\begin{aligned} CN &\leq \sum_{n=4}^{\infty} \sigma(n-1) + \sum_{n=6}^{\infty} \sigma(n-1) + \cdots \sum_{n=2W}^{\infty} \sigma(n-1) \\ &= \sum_{n=4}^{2W} \lfloor \frac{n}{2} \rfloor \cdot \sigma(n-1) + \sum_{n=2W+1}^{\infty} W \cdot \sigma(n-1) \ . \end{aligned} \tag{32}$$

Then the upper bound of $P\Big(\big|\{P_o\}\big| = 0\Big)$, the probability that there is no open path connecting $N_i^{(x_i,y_i)}$ and $\mathrm{Sink}_j^{(x_j,y_j)}$, is:

$$\begin{aligned} P\Big(\big|\{P_o\}\big| = 0\Big) &\leq \sum_{n=4}^{2W} \lfloor \frac{n}{2} \rfloor \cdot \sigma(n-1) \cdot q^n \ + \sum_{n=2W+1}^{\infty} W \cdot \sigma(n-1) \cdot q^n \\ &= \frac{2(3q)^4}{9} \left[\frac{3}{1-3q} + \frac{1-(3q)^{2W-3}}{(1-3q)^2} \right] \\ &\stackrel{\text{def}}{=} F(\lambda, R_{UG-AG}, R_{UG-UG}, D) \ . \end{aligned} \tag{33}$$

Therefore according to (30), the lower bound of the probability that a sensor at (x_i, y_i) connects to a fixed sink at (x_j, y_j) in a multi-hop fashion can be derived:

$$P(N_i^{(x_i,y_i)} \sim \mathrm{Sink}_j^{(x_j,y_j)}) \quad \begin{cases} \geq 1 - F(\lambda, R_{UG-AG}, R_{UG-UG}, D) \ , & \text{if } D > R_{UG-AG} \\ = 1 \ , & \text{if } D \leq R_{UG-AG} \ . \end{cases} \tag{34}$$

B. First Hit Time of the Random Walk Model

In this section, we analyze the first hit time of the random walk mobility model. Consider a round region $\mathbb{Q}[\mathbf{c}, r]$, where $\mathbf{c}$ is the position of the center and r is the radius. A point moves according to the random walk model as described in Section III-C. The initial position of the mobile point is $\mathbf{x}(0)$ and its position at time instant t is $\mathbf{x}(t)$. The first hit time $T_{\mathbb{Q}[\mathbf{c},r],\mathbf{x}(0)}$ is defined as the time instant when the mobile point first enters the region $\mathbb{Q}[\mathbf{c}, r]$ [15]. That is

$$T_{\mathbb{Q}[\mathbf{c},r],\mathbf{x}(0)} \stackrel{\text{def}}{=} \inf \Big\{ \ t \ \Big| \ \mathbf{x}(t) \in \mathbb{Q}[\mathbf{c}, r] \Big\} \ . \tag{35}$$

In the rest part of this subsection, we use $\mathbb{Q}$ to represent $\mathbb{Q}[\mathbf{c}, r]$ for concise expression. We are interested in the probability $P[T_{\mathbb{Q}} < t]$. Obviously, if $\mathbf{x}(0) \in \mathbb{Q}$, then $P[T_{\mathbb{Q}} < t] = 1$. Next we calculate $P[T_{\mathbb{Q}} < t]$ when $\mathbf{x}(0) \notin \mathbb{Q}$. First we analyze the probability that the mobile point $\mathbf{x}$ is inside the region $\mathbb{Q}$ at time instant t, $P[\mathbf{x}(t) \in \mathbb{Q}]$.

$$\begin{aligned} P[\mathbf{x}(t) \in \mathbb{Q}] =& P\Big[\mathbf{x}(t) \in \mathbb{Q} \ \Big| \ T_{\mathbb{Q},\mathbf{x}(0)} \leq t\Big] \cdot P(T_{\mathbb{Q},\mathbf{x}(0)} \leq t) \\ &+ P\Big[\mathbf{x}(t) \in \mathbb{Q} \ \Big| \ T_{\mathbb{Q},\mathbf{x}(0)} > t\Big] \cdot P(T_{\mathbb{Q},\mathbf{x}(0)} > t) \ . \end{aligned} \tag{36}$$

Obviously, $P\Big[\mathbf{x}(t) \in \mathbb{Q} \ \Big| \ T_{\mathbb{Q},\mathbf{x}(0)} > t\Big] = 0$. Due to the symmetric property of the random walk model, $P\Big[\mathbf{x}(t) \in \mathbb{Q} \Big| T_{\mathbb{Q},\mathbf{x}(0)} \leq t\Big] \leq \frac{1}{2}$. Then $P(T_{\mathbb{Q}} \leq t) \geq 2P[\mathbf{x}(t) \in \mathbb{Q}]$. Based on the above discussion and the mobility model, we obtain the lower bound of $P(T_{\mathbb{Q}[\mathbf{c},r],\mathbf{x}(0)} \leq t)$, the probability that the first hit time is smaller than t:

$$P(T_{\mathbb{Q}[\mathbf{c},r],\mathbf{x}(0)} \leq t) \quad \begin{cases} \geq \frac{1}{\pi t\sigma^2/\tau} \int_{\mathbf{x} \in \mathbb{Q}[\mathbf{c},r]} \exp\left(-\frac{\|\mathbf{x}-\mathbf{x}(0)\|^2}{2t\sigma^2/\tau}\right) d\mathbf{x} \ , & \text{if } \mathbf{x}(0) \notin \mathbb{Q} \\ = 1 \ , & \text{if } \mathbf{x}(0) \in \mathbb{Q} \ . \end{cases} \tag{37}$$

In next subsection, we will utilize the lower bound of $P(T_{\mathbb{Q}[\mathbf{c},r],\mathbf{x}(0)} \leq t)$ as obtained in (37).

In Section V, the upper bound of $P(T_{\mathbb{Q}[\mathbf{c},r],\mathbf{x}(0)} \leq t)$ is also needed. Hence we analyze the upper bound as follows. First we assume that $\mathbf{x}(0) \notin \mathbb{Q}$. Then we define another round region $\mathbb{Q}'[\mathbf{c}', r]$, where the center $\mathbf{c}'$ satisfies $\|\mathbf{c}' - \mathbf{x}(0)\| = r$. We analyze (36) again. It is easy to prove that

$$P\Big[\mathbf{x}(t) \in \mathbb{Q} \Big| T_{\mathbb{Q},\mathbf{x}(0)} \leq t\Big] \geq P[\mathbf{x}(t) \in \mathbb{Q}'] \stackrel{\text{def}}{=} \xi \ ,$$

where, $P[\mathbf{x}(t) \in \mathbb{Q}']$ is a determined value if the region radius r is determined. We use ξ to represent this value. Then

$$P(T_{\mathbb{Q}} \leq t) \leq \frac{1}{\xi} P[\mathbf{x}(t) \in \mathbb{Q}] \ .$$

Therefore, the upper bound of $P(T_{\mathbb{Q}[\mathbf{c},r],\mathbf{x}(0)} \leq t)$, the probability that the first hit time is smaller than t, is:

$$P(T_{\mathbb{Q}[\mathbf{c},r],\mathbf{x}(0)} \leq t) \quad \begin{cases} \leq \frac{1}{2\xi\pi t\sigma^2/\tau} \int_{\mathbf{x} \in \mathbb{Q}[\mathbf{c},r]} \exp\left(-\frac{\|\mathbf{x}-\mathbf{x}(0)\|^2}{2t\sigma^2/\tau}\right) d\mathbf{x} \ , & \text{if } \mathbf{x}(0) \notin \mathbb{Q} \\ = 1 \ , & \text{if } \mathbf{x}(0) \in \mathbb{Q} \ . \end{cases} \tag{38}$$

C. Lower Bound of the Connectivity Probability in WUSNs

Now we go back to (28) and continue to deduce the formula using the results from Section IV-A and B. The mobility of all m mobile sinks are assumed to be independent and with the same distribution parameters. Then $P(l_{mobi,\mathbf{K_{min}}} > R_{UG-AG})$ in (28) can be derived as:

$$\begin{aligned} P(l_{mobi,\mathbf{K_{min}}} > R_{UG-AG}) &= P(\min\{l_{mobi,\mathbf{K}}, \mathbf{K} \in \{M_i\}\} > R_{UG-AG}) \\ &= P(l_{mobi,\mathbf{K}} > R_{UG-AG}, \forall \mathbf{K} \in \{M_i\}) \\ &= \prod_{\mathbf{K} \in \{M_i\}} P(l_{mobi,\mathbf{K}} > R_{UG-AG}) \\ &= P^m(l_{mobi,\mathbf{K}} > R_{UG-AG}) \ . \end{aligned} \tag{39}$$

The probability $P(l_{mobi,\mathbf{K}} > R_{UG-AG})$ in (39) can be represented by the probability of the first hit time:

$$P(l_{mobi,\mathbf{K}} > R_{UG-AG}) = 1 - P(T_{\mathbb{Q}[(\mathbf{x_i},\mathbf{y_i}),R_{UG-AG}],\mathbf{K}(0)} \leq t_s) \ , \tag{40}$$

where $\mathbf{K}(0)$ is the initial position of the AG mobile sink $\mathbf{K}$ which is uniformly distributed inside the region $\mathbb{R}^2$. Therefore,

$$P(l_{mobi,\mathbf{K}} > R_{UG-AG}) = 1 - \int_{\mathbb{R}^2} \frac{1}{S_{\mathbb{R}^2}} P(T_{\mathbb{Q}[(\mathbf{x_i},\mathbf{y_i}),R_{UG-AG}],(x,y)} \le t_s)\ dxdy \stackrel{\text{def}}{=} G\left[t_s, \sigma^2/\tau, R_{UG-AG}, (x_i, y_i)\right] . \quad (41)$$

By substituting (34) and (41) into (28), we derive the lower bound of the connectivity probability of a certain UG sensor located at (x_i, y_i), which is

$$P(N_i^{(x_i,y_i)} \text{ is connected}) \quad (42)$$
$$\begin{cases} \ge \left[1 - F(\lambda, R_{UG-AG}, R_{UG-UG}, l_{fix})\right] \cdot G^m\left[t_s, \sigma^2/\tau, R_{UG-AG}, (x_i, y_i)\right] \\ \qquad + 1 - G^m\left[t_s, \sigma^2/\tau, R_{UG-AG}, (x_i, y_i)\right], & \text{if } l_{fix} > R_{UG-AG} \\ = 1, & \text{if } l_{fix} \le R_{UG-AG} . \end{cases}$$

Note that since the positions of the fixed AG sinks are determined, the minimum distance l_{fix} between N_i and all AG sinks is determined by the position of N_i, (x_i, y_i). Since $F(\lambda, R_{UG-AG}, R_{UG-UG}, l_{fix}) \ge 0$, the probability $P(T_{\mathbb{Q}[(\mathbf{x_i},\mathbf{y_i}),R_{UG-AG}],(x,y)} \le t_s)$ in $G\left[t_s, \sigma^2/\tau, R_{UG-AG}, (x_i, y_i)\right]$ is calculated using the lower bound shown in (37). For concise expression, we define:

$$F(\lambda, R_{UG-AG}, R_{UG-UG}, l_{fix}) \stackrel{\text{def}}{=} F ;$$
$$G\left[t_s, \sigma^2/\tau, R_{UG-AG}, (x_i, y_i)\right] \stackrel{\text{def}}{=} G .$$

By substituting (42) into (17) and (18), the lower bound of the connectivity probability in WUSNs is derived as:

$$P_c \ge \exp\left\{\lambda S_{fix} - \lambda S_{\mathbb{R}^2} + \lambda \int_{S_{\mathbb{R}^2} - S_{fix}} \left[(1-F)\cdot G^m + 1 - G^m\right]\ dx_i dy_i\right\} . \quad (43)$$

V. Upper Bound of the Connectivity Probability in WUSNs

The absence of isolated UG sensor is a necessary but not sufficient condition for the full connectivity in WUSNs. Hence the probability that there are no isolated UG sensors, denoted by P(no isolated UG sensor), is an upper bound for the connectivity probability in WUSNs. Therefore we have:

$$P_c \le P(\text{no isolated UG sensor}) = \sum_{n=0}^{\infty} P(\text{All } n \text{ UG sensors are not isolated}) \times P(\text{There are } n \text{ UG sensors in } \mathbb{R}^2) . \quad (44)$$

The isolation events of each node can be viewed as independent according to [8], [9]. Hence

$$P(\text{no isolated UG sensor}) = \sum_{n=0}^{\infty} P^n(N_i \text{ is not isolated}) \times P(\text{There are } n \text{ UG sensors in } \mathbb{R}^2) .$$

Then using the same strategy in (16) and (17), we derive:

$$P_c \le \exp\left\{-\lambda\, S_{\mathbb{R}^2} \cdot P(N_i \text{ is isolated})\right\} . \quad (45)$$

To derive the upper bound of P_c in (45), we analyze the lower bound of the probability $P(N_i$ is isolated). A UG sensor is isolated, if and only if no other UG sensors, AG fixed sinks and AG mobile sinks exist inside its transmission range. Since the above three events are independent, then,

$$\begin{aligned} &P(N_i \text{ is isolated}) \\ &= P(\text{no sensor, fixed sink, mobile sink inside } N_i\text{'s range}) \\ &= P(\text{no other sensor inside } N_i\text{'s range}) \\ &\qquad \times P(\text{no mobile sink inside } N_i\text{'s range}) \\ &\qquad \times P(\text{no fixed sink inside } N_i\text{'s range}) . \end{aligned} \quad (46)$$

According to the properties of the homogeneous Poisson point process, the three probabilities in (46) are calculated respectively in the following.

$$\begin{aligned} &P(\text{no other sensor inside } N_i\text{'s range}) \quad (47) \\ &= P(N_i \text{ has no sensor neighbor}) = \exp(-\lambda\pi R_{UG-UG}^2) . \end{aligned}$$

$$\begin{aligned} &P(\text{no mobile sink inside } N_i\text{'s range}) \quad (48) \\ &= P(\text{no mobi sink moves into } N_i\text{'s range within } t_s) \\ &= \left[1 - P(\text{mobi sink } M_j \text{ moves into } N_i\text{'s range within } t_s)\right]^m \\ &= \int_{S_{\mathbb{R}^2}} \int_{S_{\mathbb{R}^2}} \left(\frac{1}{S_{\mathbb{R}^2}}\right)^2 \left[1 - P(T_{\mathbb{Q}[(\mathbf{x_i},\mathbf{y_i}),R_{UG-AG}],(x,y)} \le t_s)\right]^m dxdydx_i dy_i \\ &\stackrel{\text{def}}{=} H(m, R_{UG-AG}, \sigma^2/\tau, t_s) . \end{aligned}$$

$$P(\text{no fixed sink inside } N_i\text{'s range}) = 1 - \frac{S_{fix}}{S_{\mathbb{R}^2}} . \quad (49)$$

In (48), $P(T_{\mathbb{Q}[(\mathbf{x_i},\mathbf{y_i}),R_{UG-AG}],(x,y)} \le t_s)$ is calculated using its upper bound given in (38) in order to derive the upper bound of the connectivity probability. By substituting (46)-(49) into (45), the upper bound of the connectivity probability in WUSNs is obtained.

$$P_c \le \exp\left\{-\lambda \cdot e^{-\lambda\pi R_{UG2UG}^2} \cdot (S_{\mathbb{R}^2} - S_{fix}) \cdot H(m, R_{UG2AG}, \sigma^2/\tau, t_s)\right\} . \quad (50)$$

VI. Performance Evaluation

As shown in (43) and (50), the lower and upper bounds of the connectivity probability in WUSNs are functions of various parameters, such as the UG sensor node density λ, the number n of AG fixed sinks, the number m of AG mobile sinks, the mobility of the mobile sinks σ^2/τ, the transmission ranges (R_{UG-UG}, R_{UG-AG} in sensing phase and R_{UG-UG}, R_{AG-UG} in control phase), and the tolerable latency (t_s in the sensing phase and t_c in the control phase). Moreover, as shown in Section III-A, the transmission ranges are functions of the operating frequency, the UG sensor burial depth, the AG sink antenna height, the composition of soil in terms of sand and clay fractions, the bulk density, and the soil moisture. In this section, we numerically analyze the effects of the above environmental and system parameters on the connectivity in WUSNs. The theoretical probability bounds are validated by the simulations in the meantime. All the analysis is based on the sensing phase unless otherwise specified.

Except studying the effect of certain parameters, the default values are set as follows: The sensing region is a 100 m×100 m square. The number of the UG sensor node is calculated by multiplying the region area by the sensor node density. 12 fixed AG sinks are uniformly deployed along the border of the region (3 on each square edge). 10 mobile AG sinks move inside the region according to random walk model

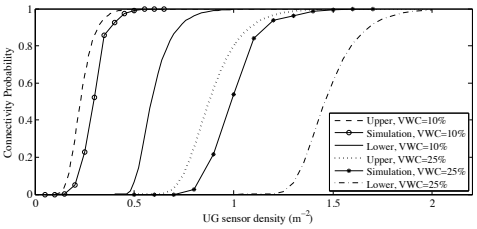

Fig. 4. Connectivity probability in WUSNs as a function of UG sensor node density with different soil moisture.

with parameter $\sigma^2/\tau = 1\ m^2/s$. The tolerable latencies are $t_s = 30$ sec in the sensing phase and $t_c = 20$ min in the control phase. All the transceivers in sensors and sinks are assumed to be the same. The transmitting power is 10 mW at 900 MHz. The minimum received power for correct demodulation is -90 dBm. The antenna gains $g_t = g_r = 5$ dB. The UG sensor burial depth is 0.5 m and the AG sink antenna height is 1 m. The volumetric water content (VWC) in the soil is 10%. The sand particle percent is 50%. The clay percent is 15%. The bulk density is 1.5 grams/cm^3, and the solid soil particle density is 2.66 grams/cm^3. Each simulation result is averaged over 500 iterations. The lower and upper bounds are calculated by (43) and (50) respectively.

A. Soil Moisture

The effects of soil moisture on the WUSNs' connectivity are illustrated in Fig. 4. The connectivity probabilities are given as a function of UG sensor node density in dry soil medium and wet soil medium, respectively. For the dry soil medium, we set VWC as 10%. For the wet soil medium, we set VWC as 25%. It indicates that the connectivity in WUSNs highly depends on the soil moisture. To achieve equal connectivity probability, the UG sensor node density of the WUSN in wet soil is more than twice of the density required in dry soil. This is because the transmission ranges of both the UG-UG and the UG-AG channel are significantly reduced when the water content in the soil increases. Since the soil moisture in the nature varies from time to time, the connectivity of the WUSNs is also dynamic.

B. Number of Fixed and Mobile Sinks

In Fig. 5, the effects of AG sink number on the WUSNs' connectivity are investigated. Specifically, we reduce the number of AG fixed sinks from 12 to 1 in Fig. 5(a), while we reduce the number of AG mobile sinks from 10 to 1 in Fig. 5(a). It is shown in the figures that the connectivity probabilities decreases if we reduce the number of AG fixed or mobile sinks. However, since the fixed sensor can only be deployed along the field border. Consequently, if there are already sufficient fixed sinks, more fixed sinks cannot provide more covered area hence cannot increase the connectivity probability. Fig. 5(a) and Fig. 5(b) also show that, if more fixed or mobile sinks are added to the network, the lower bound of the connectivity probability increases much more dramatically than the higher bound. Consequently, the UG sensor node density to fulfill the sufficient condition of the full connectivity in WUSNs is significantly reduced if more fixed or mobile sinks are introduced.

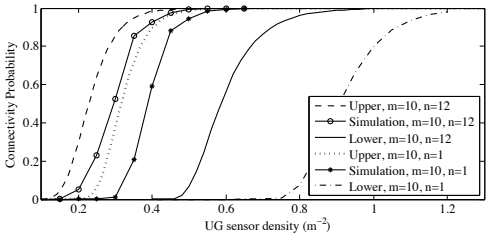

(a)

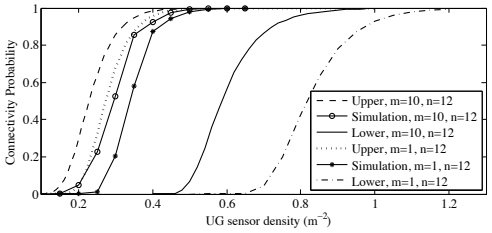

(b)

Fig. 5. Connectivity probability in WUSNs as a function of UG sensor node density with different number of (a) AG fixed sinks and (b) AG mobile sinks.

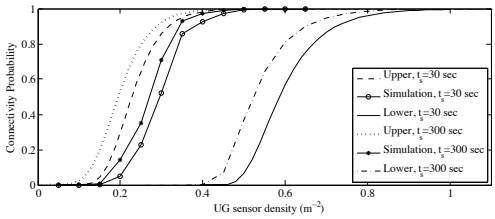

Fig. 6. Connectivity probability in WUSNs as a function of UG sensor node density with different tolerable latency.

C. Tolerable Latency and Mobility Model

Fig. 6 shows the effect of tolerable latency on the network connectivity. If we allow longer tolerable latency (from 30 sec to 300 sec), the connectivity probability increases. Therefore, there exists a tradeoff between the lower latency and higher connectivity probability. It should be noted that the effects of the mobility model's parameter σ^2/τ is similar to the tolerable latency here, which can be explained as follows. The current position of a mobile sink depends on the product of the elapsed time t and the model parameter σ^2/τ, as discussed in Section III-C. Hence, the tolerable latency and model parameter σ^2/τ have equal effects in determining whether the mobile sink can move into the range of a sensor.

D. Sensing Phase and control Phase

Due to the asymmetrical channel between the UG sensor and AG sinks, the connectivity performances of the sensing phase and the control phase are different, as shown in Fig. 7. If the tolerable latency of the two phases are the same, as illustrated in Fig. 7(a), the connectivity probability of the control phase is much lower than that of the sensing phase. It is because the transmission range of the AG-UG channel is much smaller than the UG-AG channel. Actually, the tolerable latency in the control phase can be much larger than in the sensing phase, since the sinks do not need to send control messages to the sensors frequently in most WUSNs'

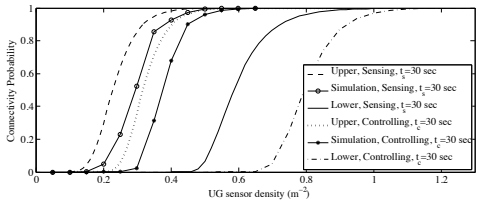

(a)

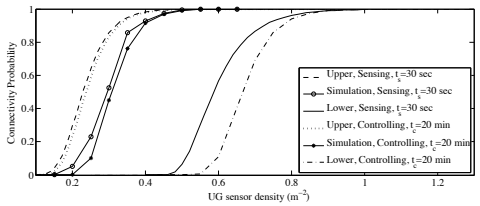

(b)

Fig. 7. Connectivity probabilities in sensing phase and control phase with different tolerable latency. (a) t_c = 30 sec. (b) t_c = 20 min.

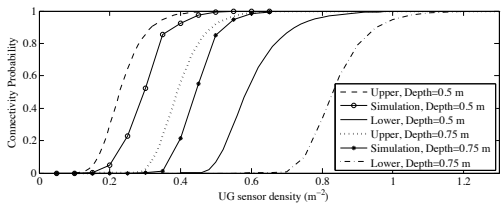

(a)

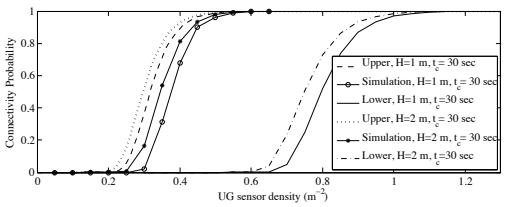

(b)

Fig. 8. Connectivity probabilities with (a) different UG sensor burial depth in sensing phase, and (b) different AG sink antenna height in control phase.

applications. Fig. 7(b) shows that the connectivity probabilities are almost the same for the two phases if the tolerable latency in control phase increases to 20 min.

E. UG Sensor Burial Depth and AG Sink Antenna Height

The effects of the UG sensor burial depth and AG sink antenna height are analyzed in Fig. 8. As discussed in Section III-B and C, both the UG-AG channel and the AG-UG channel are significantly affected by the UG sensor burial depth. Meanwhile, only the AG-UG channel is influenced dramatically by the AG sink antenna height. Hence the effects of sensor burial depth is analyzed in the sensing phase in Fig. 8(a), and the effects of sink antenna height is analyzed in the control phase in Fig. 8(b). In Fig. 8(a), the connectivity probability bounds drop dramatically after the sensor burial depth increases only 0.25 m. Meanwhile, the connectivity probability bounds only increase a little when the sink antenna height is doubled.

VII. Conclusions

The soil transmission medium makes the WUSNs different from the terrestrial wireless sensor networks. Due to the unique channel characteristics, such as high path loss in soil medium and the reflection/refraction on the air-ground interface, a heterogeneous network structure, which consists of UG sensor, AG fixed sink and AG mobile sink, is required in WUSNs. In this paper, the probabilistic connectivity of such WUSNs is investigated. The upper and lower bounds of the connectivity probability are theoretically developed to provide the necessary and sufficient conditions to achieve the full-connected network, which give the guidelines to design the system parameters of the WUSNs according to the environmental conditions. The theoretical bounds are validated by simulations in various scenarios with different system and environmental parameters. Our analysis shows that the UG sensor density, the soil moisture content, and the UG sensor burial depth are the three parameters that have the most significant effects on the connectivity. Other parameters that have obvious effects include: the number and the mobility of the AG sinks, the tolerable latency, and the AG sink antenna height.

Acknowledgment

This work is based upon work supported by the US National Science Foundation (NSF) under Grant No. CCF-0728889.

References

[1] I. F. Akyildiz and E. P. Stuntebeck, "Wireless underground sensor networks: Research challenges," *Ad Hoc Networks Journal (Elsevier)*, vol. 4, pp. 669-686, July 2006.

[2] I. F. Akyildiz, Z. Sun and M. C. Vuran, "Signal Propagation Techniques for Wireless Underground Communication Networks," *Physical Communication Journal (Elsevier)*, Vol. 2, No. 3, pp.167-183, September 2009.

[3] H. R. Bogena, J. A. Huisman, H. Meier, U. Rosenbaum, and A. Weuthen, "Hybrid Wireless Underground Sensor Networks: Quantification of Signal Attenuation in Soil," *Vadose Zone J.*, vol. 8, no. 3, pp. 755-761, August 2009.

[4] J. Tiusanen, "Wireless Soil Scout prototype radio signal reception compared to the attenuation model," *Precision Agriculture*, DOI 10.1007/s11119-008-9096-7, November 2008.

[5] L. Li, M. C. Vuran, and I. F. Akyildiz, "Characteristics of Underground Channel for Wireless Underground Sensor Networks," in *Proc. IFIP Mediterranean Ad Hoc Networking Workshop (Med-Hoc-Net '07)*, Corfu, Greece, June 2007.

[6] A. R. Silva and M. C. Vuran, "Development of a Testbed for Wireless Underground Sensor Networks," *EURASIP Journal on Wireless Communications and Networking (JWCN)*, vol. 2010, Article ID 620307, 2010.

[7] P. Gupta and P. R. Kumar, "Critical Power for Asymptotic Connectivity," in *Proc. IEEE CDC*, Tampa, USA, December 1998.

[8] C. Bettstetter, "On the Minimum Node Degree and Connectivity of a Wireless Multihop Network," in *Proc. ACM MOBIHOC*, Lausanne, Switzerland, June 2002.

[9] P. Santi and D. M. Blough , "The Critical Transmitting Range for Connectivity in Sparse Wireless Ad Hoc Networks," in *IEEE Trans. Mobile Computing*, vol.2, no.1, pp. 25-39, 2003.

[10] O. Dousse, P. Thiran and M. Hasler, "Connectivity in Ad-Hoc and Hybrid Networks," in *Proc. IEEE INFOCOM*, New York, June 2002.

[11] O. Dousse, P. Mannersalo, P. Thiran, "Latency of Wireless Sensor Networks with Uncoordinated Power Saving Mechanisms," in *Proc. ACM MOBIHOC*, Tokyo, Japan, May 2004.

[12] F. Fabbri and R. Verdone, "A Statistical Model for the Connectivity of Nodes in a Multi-Sink Wireless Sensor Network Over a Bounded Region," in *Proc. European Wireless Conference (EW'08)*, Prague, Czech Republic, June 2008.

[13] T. Camp, J. Boleng and V. Davies, "A Survey of Mobility Models for Ad Hoc Network Research," *Wireless Communications and Mobile Computing*, vol.2, no.5, pp. 483-502, September 2002.

[14] R. Meester and R. Roy, *Continuum percolation*, Cambridge University Press, 1996.

[15] J. Medhi, *Stochastic processes*, 2nd ed. New York : J. Wiley, 1994.